Applied Clay Science 161 (2018) 119–126

Contents lists available at ScienceDirect

Applied Clay Science

journal homepage: www.elsevier.com/locate/clay

Research paper

Mineral carbonation of ceramic brick at low pressure and room temperature. A simulation study for a superficial CO_2 store using a common clay as sealing material

Domingo Martín*, Patricia Aparicio, Emilio Galán

Departamento de Cristalografía, Mineralogía y Química Agrícola, Universidad de Sevilla, Spain

ARTICLE INFO

Keywords:
Mineral carbonation
Mineral sequestration
Carbon capture and storage
Ceramic bricks
Common clay
Sealing rock

ABSTRACT

This research explores the possibilities of CO_2 sequestration on ceramic bricks in a short time and at surface conditions. The experiment was carried out in a specially designed reaction chamber, filled with brick wastes and sealed with common clays. The brick used were composed of quartz, wollastonite, diopside, orthoclase and anhydrite, and the common clay was a marl composed of calcite, quartz, illite, smectite and kaolinite. Experimental condition in the reaction chamber were: reaction time 5 months, pressure of CO_2 0.5 bar, 4:1 solid/water ratio. The experiment was followed by XRD, XRF, BET, physical sorption by N_2 and CO_2, Hg porosity, TG-DTA, SEM and ICP-EOS.

After the CO_2 treatment, wollastonite and anhydrite were practically destroyed and some diopside and orthoclase. Calcite precipitated as new phase (up to 48 wt%), and small amount of illite was the result of orthoclase alteration.

Concerning the sealing clay, the CO_2 produced an increment of calcite content (from 32 to 41 wt%) and a partial destruction of smectite, particularly close to the upper part of the brick layer.

These results are hopeful in relation with the possible mineral carbonation of building ceramic waste in a short time at surface conditions, and open the opportunity to use those wastes for CO_2 trapping in an appropriate system, as a quarry reclamation.

1. Introduction

It is well known the urgent necessity for reducing the emission of anthropogenic greenhouse gases that produce dramatic effects on the Climate Change. Generally, human activities result in emissions of principal greenhouses gases (GHG): CO_2, CH_4, NO_x and halocarbons. All these GHG have increased from the pre-industrial era until nowadays, and particularly CO_2 increased around 40% as a direct consequence of the fossil fuel consumption and the change of soil use (Metz et al., 2005; Stocker et al., 2013). In order to avoid the potentially devastating consequences of global warning and climate change, the anthropogenic CO_2 emissions should be reduced. Main proposed measures lead to reduce the consumption of energy from burning fossil fuels and replacing them with “clean” energy such as renewables, and the use of technologies of capture, transport and storage of CO_2. Such strategy involves the development of innovate, available and cost-effective carbon capture and storage (CCS) technologies.

The storage of CO_2 may be carried out through a number of mechanisms, including mineral carbonation, oceanic storage, underground injection for enhance fossil fuel recovery, and injection into saline aquifers (Giammar et al., 2005; Metz et al., 2005).

Carbon dioxide sequestration by mineral carbonation mimics the naturally occurring rock weathering. The rock weathering has played an important role in the historical reduction of CO_2 concentration in the atmosphere. In this process, CO_2 and water play an important role to dissolve unstable rock-forming minerals releasing alkali and alkaline-earths cations and forming phyllosilicates and carbonates. The mineral carbonated process as an alternative for CO_2 sequestration was originally proposed by Seifritz (Seifritz, 1990). The principal benefit of this process is that the formed carbonates as final products are stable over geological time periods. However, as the weathering is a very slow process, the carbonation of silicates must be accelerated to be considered as a good CO_2 sequestration alternative.

Several investigations on magnesium- or calcium-based rock-forming minerals have been carried out as potential sources for fixing CO_2 by conversion to carbonated, e.g. olivine, serpentine and wollastonite, and, despite those silicates are not very abundant in the Earth, the mineralogical carbon sequestration could contribute significantly to

* Corresponding author.
E-mail address: dmartin5@us.es (D. Martín).

https://doi.org/10.1016/j.clay.2018.04.021
Received 20 February 2018; Received in revised form 11 April 2018; Accepted 13 April 2018
Available online 24 April 2018

Table 1
Chemical composition of original and treated samples (wt%) by XRF; normalized at 100 wt%.

Sample	SiO_2	Al_2O_3	Fe_2O_3	MnO	MgO	CaO	Na_2O	K_2O	TiO_2	P_2O_5	SO_3	LOI	TOTAL
Brick	50.6	11.0	4.4	0.1	2.0	23.8	0.5	2.1	0.6	0.2	1.3	3.6	100.0
Marl	39.8	12.1	5.4	0.1	2.3	16.8	0.6	2.1	0.6	0.1	2.3	17.8	100.0
Marl 0–5 cm	41.2	12.4	5.0	0.1	2.3	16.3	0.7	2.1	0.6	0.2	1.8	17.3	100.0
Marl 5–10 cm	41.1	12.3	5.1	0.1	2.3	16.3	0.6	2.1	0.6	0.2	2.0	17.4	100.0
Marl 10–15 cm	40.8	12.3	4.9	0.1	2.3	16.5	0.6	2.1	0.6	0.2	1.7	17.9	100.0
Marl 15–20 cm	39.9	12.2	5.0	0.1	2.4	17.1	0.7	2.1	0.6	0.2	1.8	18.0	100.0
Marl 20–25 cm	38.7	11.8	4.7	0.1	2.4	18.5	0.6	2.1	0.6	0.2	1.4	18.9	100.0
Marl 25–30 cm	36.4	11.2	4.5	0.1	2.5	20.4	0.6	2.0	0.6	0.2	1.0	20.6	100.0
Brick layer (5 cm)	45.6	9.5	3.9	0.1	1.5	21.6	0.4	1.5	0.5	0.2	0.3	15.0	100.0
Marl at the bottom (5 cm)	40.2	12.0	4.8	0.1	2.2	17.1	0.6	2.0	0.6	0.2	1.6	18.8	100.0
Detection Limit (DL)	0.01	0.01	0.01	0.02	0.01	0.04	0.01	0.02	0.03	0.01	0.22		
Quantification Limit (QL)	0.02	0.02	0.02	0.03	0.02	0.05	0.03	0.03	0.10	0.02	0.23		
Relative Error	0.012	0.020	0.058	0.184	0.007	0.047	0.038	0.028	0.061	0.025	0.063		

LOI: Loss on ignition.

Table 2
Mineralogy composition of original and treated samples (wt%) by XRD.

Sample	Quartz	Wollastonite	Diopside	Orthoclase	Anhydrite	Calcite	Dolomite	Illite	Smectite	Kaolinite
Brick	15	35	25	18	7					
Marl	10					25	tr	17	34	13
Marl 15–20 cm	10					26	tr	18	32	13
Marl 20–25 cm	10					27	tr	19	29	14
Marl 25–30 cm	9					29	tr	19	28	14
Brick layer (5 cm)	18	6	9	7	2	48	tr	10		
Marl at the bottom (5 cm)	9					28	tr	19	29	14

tr: traces.

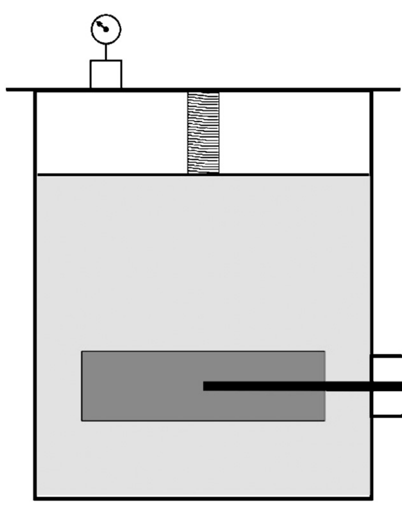

Fig. 1. Scheme of the reaction chamber designed for CO_2 brick reaction. In dark grey is represented the brick layer and in light grey the marl.

the CO_2 sequestration, mainly in the proximity of the emission source. This technology is called ex-situ mineral sequestration of CO_2 as it was proposed by Seifritz and studied in detail by Lackner and co-author (Lackner et al., 1995). The basic reactions, which take places after the Ca and Mg release, are exemplified by the following reactions:

$$CaO + CO_2 \rightarrow CaCO_3 + 179 \text{ kJ/mole} \tag{1}$$

$$MgO + CO_2 \rightarrow MgCO_3 + 118 \text{ kJ/mole} \tag{2}$$

Until now the experiments conducted for the carbonation of magnesium silicates (olivine and serpentine) via magnesium oxide or magnesium hydroxide intermediates, were carried out at high temperature and pressure, 600 °C and 100 bar (allowing for both sub- and supercritical conditions for CO_2) (Fagerlund et al., 2009), or under hydrothermal conditions, in the case of anorthite (Hangx and Spiers, 2009). But these conditions are not very economic, and they are weak points of the accelerated carbonation studies.

In addition, an industrial-scale operation may require the mining and grinding of suitable Mg- and Ca-bearing silicate minerals to accelerate the carbonation process, making the process not economically and environmentally viable.

For these reasons, several authors used other source of Mg and Ca such is the case of Mg- or Ca- containing mine tailings and by-products or waste from industry for carbonation. Such is the case of the carbonation of fly-ash (Montes-Hernandez et al., 2009), steel making slag (Huijgen et al., 2005), asbestos-mining tailings, electric arc furnace (EAF) dust, cement-kiln dust (Huntzinger et al., 2009), waste concrete (Shao et al., 2006), air pollution control (APC) residues (Baciocchi et al., 2006), etc.

This research explores the possibilities of CO_2 sequestration on ceramic bricks by mineral carbonation in a short time and at surface conditions. The results could be used for carbonation of ceramic wastes, at an industrial scale, particularly if such wastes were used as reclamation materials for filling exhausted quarries, in which the CO_2 could be injected. In this way, moreover the role of a possible sealing rock (common clay) was also investigated.

2. Materials and methods

2.1. Raw materials and carbonation experiment

The bricks (AUC1) used for carbonation come from La Puebla de Cazalla (Sevilla, Spain), and were fired at 900 °C. Such bricks were selected because of their high calcium content (Table 1), which can be releases after the CO_2 attack in presence of water. The brick is mainly composed of quartz, diopside, wollastonite and orthoclase, and minor anhydrite (Table 2). This brick was carbonated in an early study (Martín et al., 2016), producing calcite from the partial destruction of silicates and anhydrite. In that previous study, the carbonation was proportional to the reaction time and was independent of the particle-size fraction. The largest quantities of carbonates were obtained for the

Fig. 2. Sampling material (core) from the reaction chamber after 5 months.

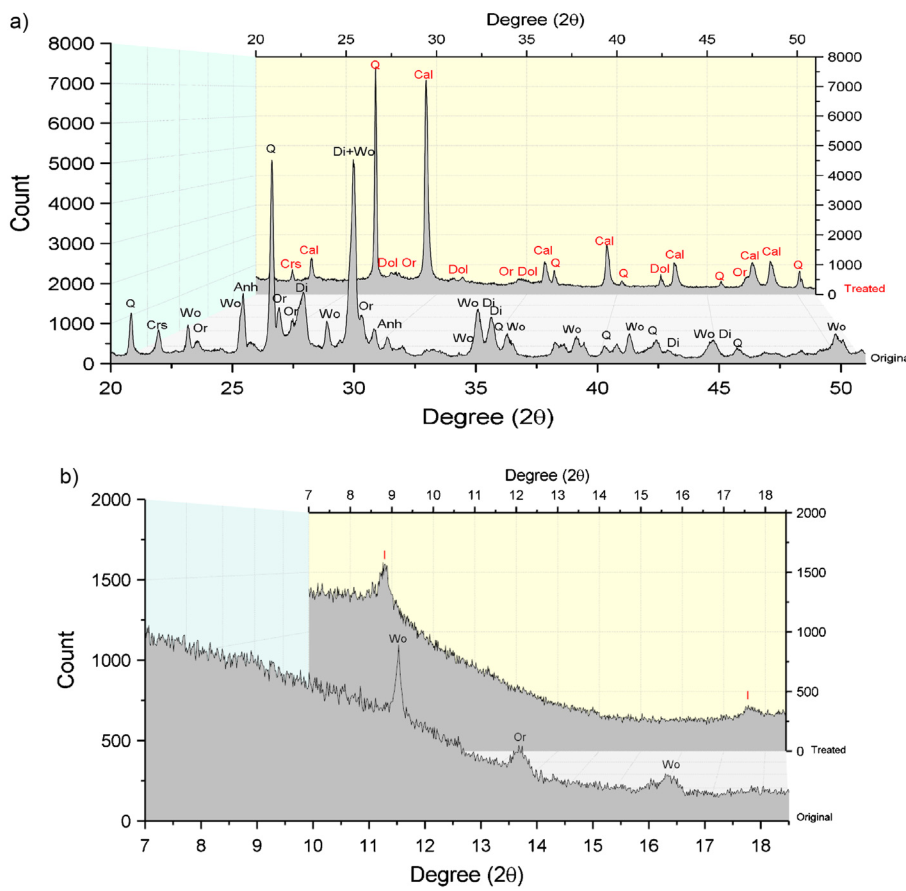

Fig. 3. XRD pattern (a) and low angle (b) of original and treated brick. Abbreviations: Q: quartz, Crs: cristobalite, Wo: wollastonite, Or: orthoclase, Anh: anhydrite, Di: diopside, Cal: calcite, I: illite, Dol: dolomite.

following experimental conditions: 30 days, > 4 mm fraction, 10 bar of CO_2, 4:1 solid/water ratio and room temperature.

The clay used for recovering the brick during carbonation as sealing material comes from the “blue marl” formation of the Guadalquivir Tertiary basin (S. Spain). The marl contains calcite, quartz, illite, smectite and kaolinite and trace of dolomite and the chemical composition agrees with the mineralogical composition (Tables 1 and 2).

In this experiment the carbonation of bricks was carried out in a chamber designed ad hoc (Fig. 1). The brick, previously milled, was recovered in the chamber with clays at the base, walls and at the top, in order to favour the retention of the CO_2 while the reaction occurs.

The reaction conditions were the following: 0.5 bar, 4:1 solid/water ratio and room temperature. The gas injection was controlled by a mass flow controller in order to do constant the internal CO_2 pressure. This controller was connected to a computer that registers the CO_2 injection.

The reaction time was five months. After this time a sampling was drawn and the core obtained was cut in sections of five centimetre thickness (Fig. 2). The first six sections from the top correspond to the upper marl layer, the next is the brick, and the last corresponds again to the marl at the bottom.

Table 3
Carbon content and calculated calcite, N_2-BET and Ca, K, Mg, Si and S soluble ions evolution in the original brick and marl, and their evolution with depth on the camber reactor and original brick and marl.

Sample	Depth (cm)	C content (%)	Calcite (%)	Δm (%)	N_2-BET (m^2/g)	Ca (mg/l)	K (mg/l)	Mg (mg/l)	Si (mg/l)	S (mg/l)
Brick	–	0.117	1.0	2.5	13.6	331.57	–	–	–	–
Marl	–	3.865	32.2	16.9	36.0	34.85	27.35	–	–	–
Marl 0–5 cm	0–5	3.967	33.0	17.0	38.8	32.65	27.27	9.44	8.85	203.1
Marl 5–10 cm	5–10	4.069	33.9	17.0	40.3	33.24	25.41	8.48	5.17	209.5
Marl 10–15 cm	10–15	4.017	33.4	17.6	41.6	32.52	26.54	7.30	7.10	203.3
Marl 15–20 cm	15–20	4.145	34.5	17.7	42.1	30.76	28.15	7.34	8.26	217.3
Marl 20–25 cm	20–25	4.455	37.1	18.6	42.3	25.14	31.40	5.50	7.11	219.4
Marl 25–30 cm	25–30	4.892	40.7	20.2	42.7	12.85	36.37	3.60	6.88	240.5
Brick layer (5 cm)	30–35	3.137	26.1	13.1	10.3	66.11	11.47	9.03	11.97	38.5
Marl at the bottom (5 cm)	35–40	4.123	34.3	17.9	40.8	40.93	30.86	9.54	6.24	316.9

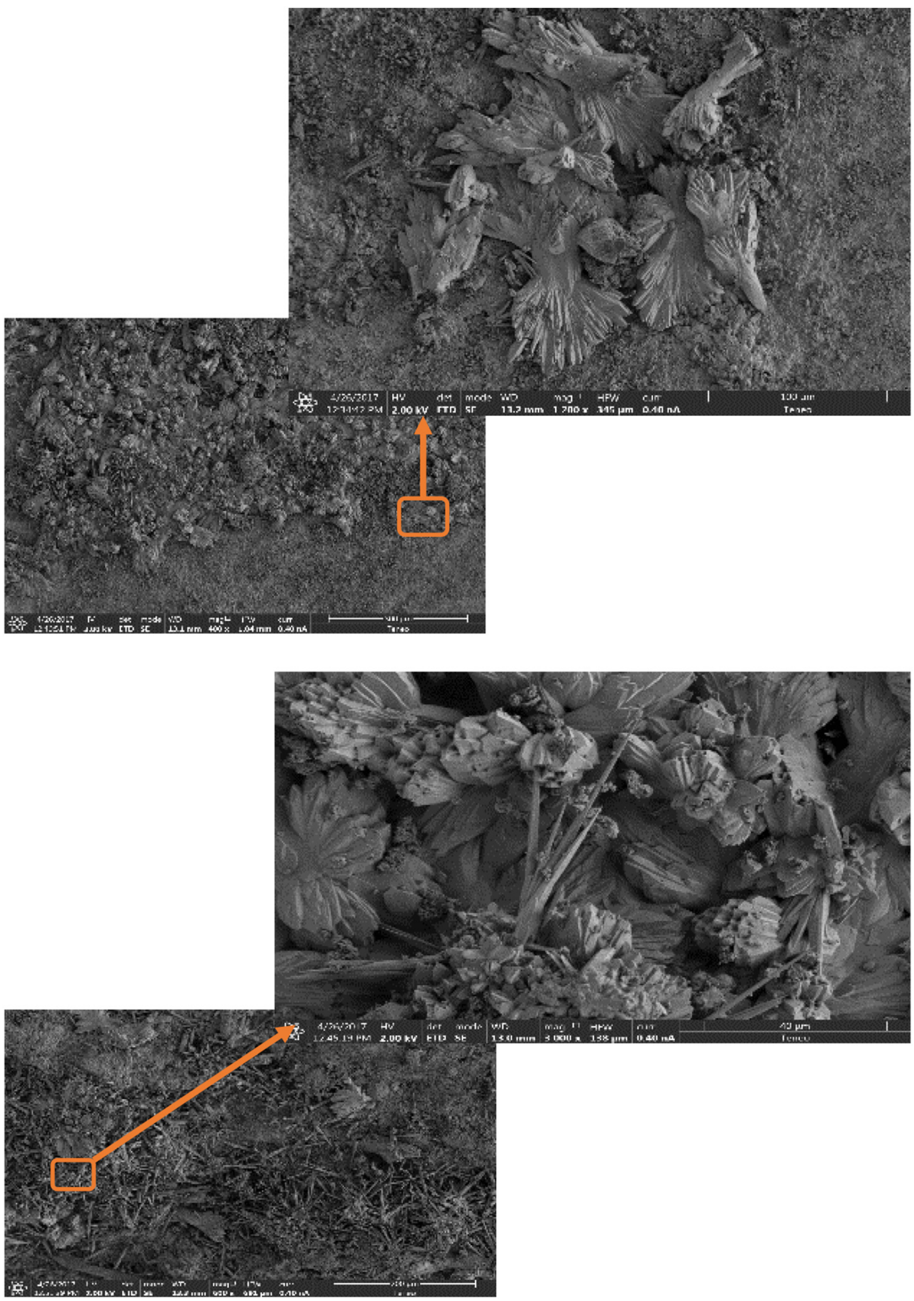

Fig. 4. Neoformed calcite crystal on the brick's surface by SEM.

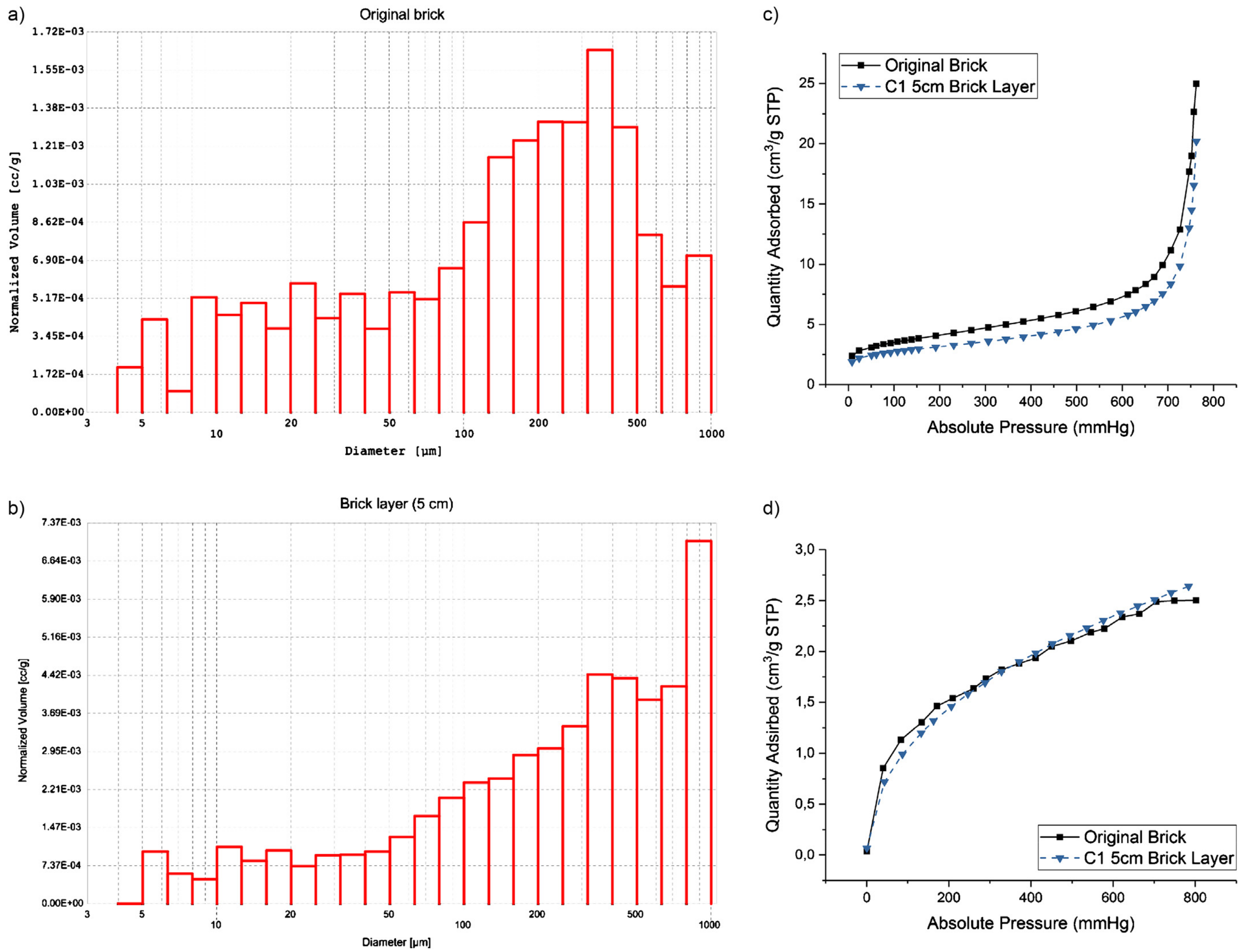

Fig. 5. a) and b) Histogram of Hg porosity, c) N_2 adsorption and d) CO_2 adsorption isotherms for original brick and treated brick layer.

Table 4
Relative humidity evolution with depth on the chamber reactor.

Sample	Depth (cm)	RH (%)
Marl 0–5 cm	0–5	13.3
Marl 5–10 cm	5–10	13.2
Marl 10–15 cm	10–15	16.8
Marl 15–20 cm	15–20	19.6
Marl 20–25 cm	20–25	20.4
Marl 25–30 cm	25–30	20.7
Brick layer (5 cm)	30–35	14.3
Marl at the bottom (5 cm)	35–40	21.5

2.2. Material characterization and carbonation process tracing

The mineralogical composition of the untreated and treated samples was determined by X-ray diffraction (XRD), using a Bruker D8 Advance diffractometer with standard monochromatic Cu Kα radiation and operating at 40 kV and 30 mA. Scanning was performed with a 0.015° 2θ step size, and at 0.1 s per step from 3° to 70°. Phyllosilicates identification was accomplished on oriented aggregates, after the standard treatments with ethylene-glycol, and heating at 550 °C for two hours.

The major elemental composition expressed in oxides was performed by X-ray fluorescence (XRF) with an automated Panalytical Axios model spectrometer. The samples were prepared for analysis as glass discs to reduce the "matrix effect".

A profile-fitting peak decomposition program, part of MacDiff 4.2.5 by Petschick (Petschick, 2010, 2004), was used to assess changes in the main representative reflexions of the XRD patterns. A Pearson VII function was used to obtain the following parameters: peak position, height above the baseline, full width at half height, and the mixing parameter for the function.

The carbonate content of carbonated samples was determined by two analytical methods: thermal analysis (TG-DTA) and elemental analyser. The TG-DTA were performed in a TG Netzsch STA 409PC. Samples (around 150 mg) were heated in aluminium oxide crucible under a nitrogen atmosphere at 10 °C min^{-1} from room temperature to 1200 °C. Mass loss was measure by TG in the range of temperature 450–900 °C relative to the total carbonated decomposition. In the case of the marl, the dehydroxilation of phyllosilicates in this range was taken into account. The elemental carbon content was measured using an elemental analyser, Leco Truspec CHNS Micro which calculates the carbonated ratio assuming that the whole carbon content was calcite.

The specific surface area (BET), micro- and nanoporosity were measured with an ASAP 2420 instrument using the absorption of N_2 at liquid nitrogen temperature (77.35 K) and CO_2 at 273 K. Prior to measuring, all the samples were degassed at 150 °C for 180 min and finally outgassed to 10^{-3} Torr. Macro- and mesoporosity were studied using a mercury porosimeter Quantachrome Instruments Pore Master 60-GT.

The analysis of soluble Ca, K, Mg, Si and S ions was performed with

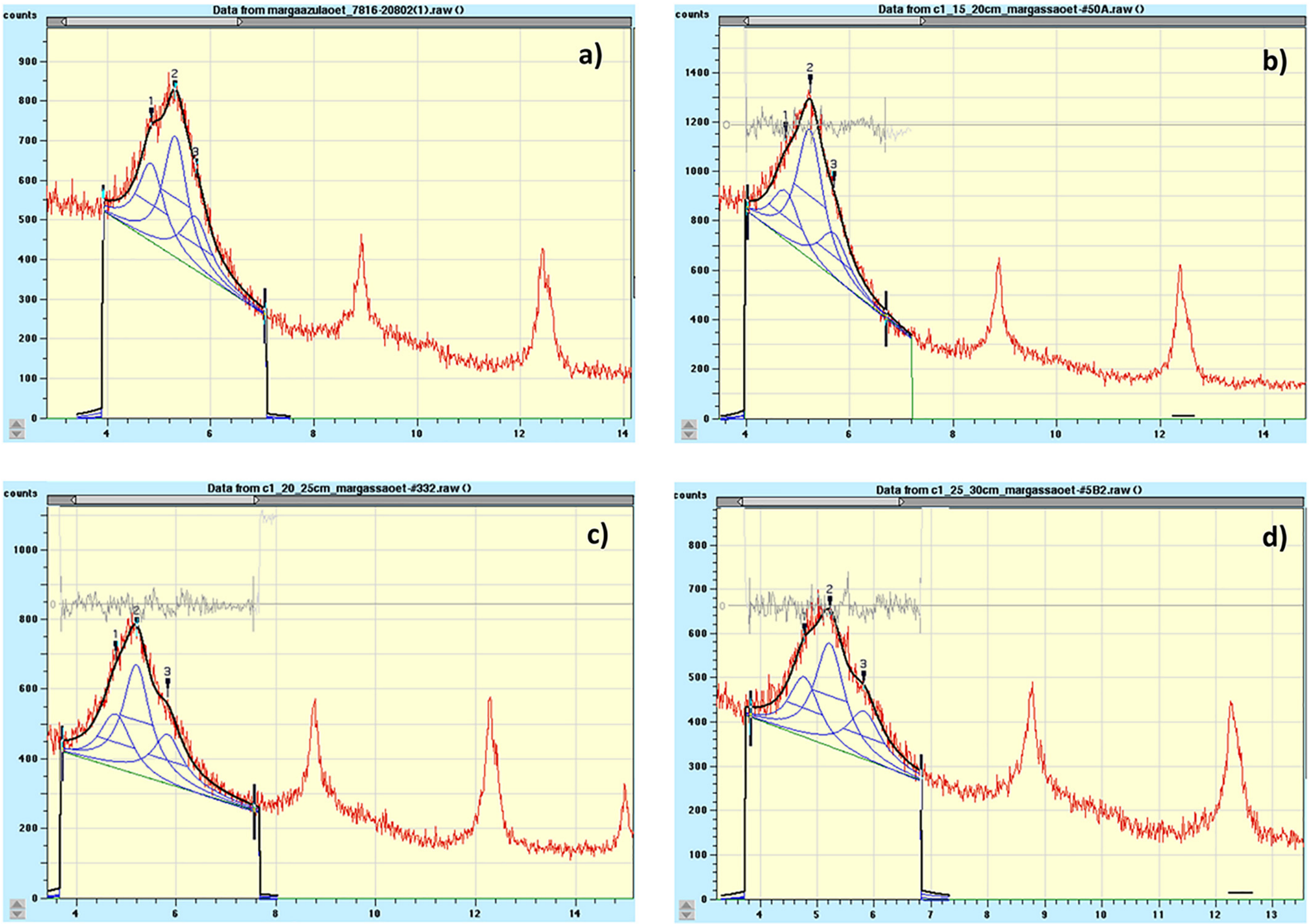

Fig. 6. Fitting XRD (a) pattern of original marl, and treated marls at different depth, (b) 15–20 cm, (c) 20–25 cm and (d) 35–30 cm.

simultaneous ICP-OES analysis using a Horiba Jobin Yvon ULTIMA 2 model instrument. The sample were prepared by mixing the solid powder samples with water and stirring for 24 h, afterwards isolating the liquid phase by centrifugation and filtered using a Nylon 0.22 μm syringe filter.

Micro observations of morphological changes were obtained by scanning electronic microscopy (SEM) using a JEOL 6460 LV microscope and FEI Teneo, both equipped with energy dispersive spectrometers (Oxford Instruments INCA and EDAX, respectively).

The moisture content of the different sections obtained from the core was measured after heating in an oven at 105 °C during 24 h.

3. Results and discussion

3.1. Mineralogical carbon sequestration by brick

The XRD patterns of the original and treated bricks are displayed in Fig. 3. The presence of calcite in treated samples is evident, as well as the practical destruction of calcium silicate (wollastonite, diopside), anhydrite and orthoclase (Fig. 3a). In addition, minor dolomite precipitated and some illite formed from the orthoclase alteration (Fig. 3b). This mineral destruction was due to the acid attack of carbonic acid produced by combination of CO_2 and water. Calcium ions released, combined with carbonic ions, precipitated as calcite. At the same time, probably the amorphous phase increased in the treated brick as it can deduced from the increase of the background of the XRD patterns. These changes are in agreement with the loss on ignition, which increased substantially due the increment on calcite content (Table 1).

The semi-quantification of carbonates by XRD, elemental carbon content and TG of treated bricks confirms that the carbonation process converts the gaseous CO_2 to solid calcium carbonate (Table 3).

New-formed calcite crystals growth on the brick's surface in different habits, such as pseudo-rhombohedral shapes and needles, or formed, in other cases, big layers of carbonate crystals, sometimes filling pores (Fig. 4). Small geometric aggregates of lamellar crystals and dendritic habit can also be observed.

Concerning the BET evolution (Table 3), there was a small decrease from the original to treated samples (from 13 to 10 m^2/g of specific surface area) probably due to calcite precipitation in micropores. Unlike, the CO_2 treatment produced an increment of macro- and mesoporosity as determined by Hg-porosity, which affects the proportion and size of the porous (Fig. 5a and b), due to the partial destruction of calcium silicates. The treated brick N_2 adsorption is lower than in the original brick (Fig. 5c), probably related to physical CO_2 retention. The CO_2 adsorption isotherms at low pressure show that adsorption was higher in original brick than in the treated brick, and vice versa at high pressure (Fig. 5d).

Brick humidity and the total calcium content of the brick decreased after the treatment (Tables 1 and 4). Moreover, soluble calcium content decreased after the treatment (Table 3), probably due to carbonate precipitation. Some of this soluble calcium could be transferred to water and migrated to the marls.

It is also known that water is necessary to promote the attack of CO_2. In presence of water the carbonation mechanism can be considered a sequential reaction expressed by the following equations (Freyssinet et al., 2002; Li et al., 2007):

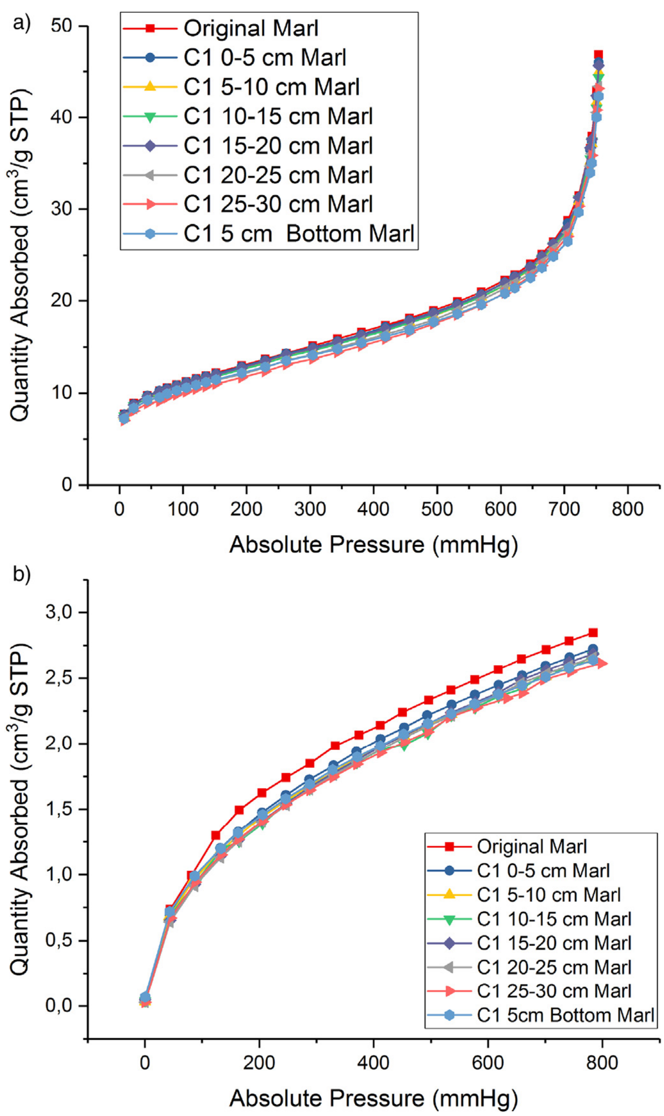

Fig. 7. (a) N_2 and (b) CO_2 absorption isotherms for original and treated marls.

$$H_2O + CO_2 \rightarrow H_2CO_3 \quad (3)$$

$$H_2CO_3 \rightarrow H^+ + HCO_3^- \rightarrow 2H^+ + CO_3^{2-} \quad (4)$$

$$Ca^{2+} + CO_3^{2-} = CaCO_3 \quad (5)$$

3.2. Behavior of sealing marl layer

Galán and Aparicio (2014) studied the effect of the CO_2 on this marl under high pressure and temperature conditions. Smectite and illite underwent some degradation, and a physical retention of CO_2 was detected.

In this experiment, the original marl humidity (13 wt%) increased particularly in contact with the brick layer (21 wt%). Likely, a water transfer by capillarity occurred from the brick during the process, and it was probably absorbed by smectite (Table 4).

At the same time, the calcite content increased while the smectite content decreased, particularly close to the brick (Table 2). These results do not agree with those obtained by Galán and Aparicio (2014), probably because they did not find carbonates after CO_2 reaction at supercritical conditions. According to the fitting done in the XRD pattern of the ethylene-glycol oriented aggregates (Fig. 6), a partial destruction and transformation of smectite in the marl close to the brick layer occurred (Fig. 6 d). This fact could deduce by a lower intensity of the reflection at 16 Å and the displacement of the d_{value}. On the contrary, in kaolinite and illite did not change after the reaction.

After the treatment the total calcium and carbon increased, especially in contact with brick layer (Tables 1, 3), due to an arise of calcite in the marl. According to Eqs. (3), (4) and (5), such increases of carbonate and humidity would be related to the possible transfer of CO_2 on the water and with an external contribution of calcium from the brick. In fact, on the brick decreases the amount of calcium content after the treatment respect to the original (Table 1).

There was not a significant variation of N_2-BET specific surface area (Table 3). On the contrary, CO_2 specific surface area evolution showed an important difference between the original sample and the treated one. In the latter, the CO_2 adsorption isotherms show less volume adsorbed in all range of pressure than the original sample (Fig. 7.). This reduction is proportional to depth, and it could be related with physical retention of CO_2 in micro- and nanoporous and/or due to the carbonate precipitation covering/filling pores.

Soluble calcium (Table 3) of the marl decreased in the first centimeters above the brick layer, but not under the brick, probably due to calcite precipitation too. On the contrary, potassium increased inversely, because of the K-feldspar alteration on the brick. There was not important variation of magnesium and silicon ions. Nevertheless, sulfur ions were concentrated close to the brick layer and especially at the bottom. This fact prevents sulfur escape to the surface.

In summary, all the results obtained show that wollastonite and a significant proportion of anhydrite were destroyed in the brick layer. In addition, a mineral transformation of potassium feldspar into illite also occurred. In the marls the most significant mineral change was the smectite destruction. Calcium released precipitates as calcite sequestering around 10 wt% of CO_2 in five months in the brick. The major proportion of CO2 captured on the marls was around 4 wt%, at the marls level close to the brick.

The CO_2 treatment produced on the brick an increment of macro-, meso- and nanoporosity and a decrease of the microporosity by the combination of two process: a) the destruction of minerals by the action of carbonic acid, that produced an irregular surface and an increment of macro and mesoporosity; and b) the precipitation of carbonates, that filled the micro-porous and probably transformed them in nanoporous. The results indicated also a physical retention of CO_2.

4. Conclusions

The present study shows the possibility of using ceramic construction residues for mineral carbonation under surface conditions in a short time, by mean of the practical destruction of all the calcium silicates. In addition, the acid attack of anhydrite can lead to a subsequent precipitation of calcium carbonate.

The designed system, that would mimic the reclamation of a quarry filled up with bricks and with marl as sealing material, was run satisfactory, fixing the CO_2 as calcite in the brick and in the marls. These results open the opportunity to use these wastes for CO_2 sequestration in a real quarry reclamation.

Acknowledgements

This research was funded by the Andalucía Government (RDCCO2 Project, P12-RNM-568), and the contract of Domingo Martín granted by the V Plan Propio de Investigación from the University of Seville (Spain). XRD, XRF, TXRF, BET, C-elemental analysis was performed using the facilities of the General Research Center at the University of Seville (CITIUS). Authors are grateful to editor and reviewers for their comments which improved the manuscript.

References

Baciocchi, R., Polettini, A., Pomi, R., Prigiobbe, V., Von Zedwitz, V.N., Steinfeld, A., 2006.

CO_2 Sequestration by Direct Gas-solid Carbonation of Air Pollution Control (APC) Residues. http://dx.doi.org/10.1021/EF060135B.

Fagerlund, J., Teir, S., Nduagu, E., Zevenhoven, R., 2009. Carbonation of magnesium silicate mineral using a pressurised gas/solid process. Energy Procedia 4907–4914. http://dx.doi.org/10.1016/j.egypro.2009.02.321.

Freyssinet, P., Piantone, P., Azaroual, M., Itard, Y., Clozel-Leloup, B., Guyonnet, D., Baubron, J.C., 2002. Chemical changes and leachate mass balance of municipal solid waste bottom ash submitted to weathering. Waste Manag. 22, 159–172. http://dx.doi.org/10.1016/S0956-053X(01)00065-4.

Galán, E., Aparicio, P., 2014. Experimental study on the role of clays as sealing materials in the geological storage of carbon dioxide. Appl. Clay Sci. 87, 22–27. http://dx.doi.org/10.1016/j.clay.2013.11.013.

Giammar, D.E., Bruant, R.G., Peters, C.A., 2005. Forsterite dissolution and magnesite precipitation at conditions relevant for deep saline aquifer storage and sequestration of carbon dioxide. Chem. Geol. 217, 257–276. http://dx.doi.org/10.1016/j.chemgeo.2004.12.013.

Hangx, S.J.T., Spiers, C.J., 2009. Reaction of plagioclase feldspars with CO_2 under hydrothermal conditions. Chem. Geol. 265, 88–98. http://dx.doi.org/10.1016/j.chemgeo.2008.12.005.

Huijgen, W.J.J., Witkamp, G.-J., Comans, R.N.J., 2005. Mineral CO_2 sequestration by steel slag carbonation. Environ. Sci. Technol. 39, 9676–9682. http://dx.doi.org/10.1021/es050795f.

Huntzinger, D.N., Gierke, J.S., Sutter, L.L., Kawatra, S.K., Eisele, T.C., 2009. Mineral carbonation for carbon sequestration in cement kiln dust from waste piles. J. Hazard. Mater. 168, 31–37. http://dx.doi.org/10.1016/j.jhazmat.2009.01.122.

Lackner, K.S., Wendt, C.H., Butt, D.P., Joyce, E.L., Sharp, D.H., 1995. Carbon dioxide disposal in carbonate minerals. Energy 20, 1153–1170. http://dx.doi.org/10.1016/0360-5442(95)00071-N.

Li, X., Bertos, M.F., Hills, C.D., Carey, P.J., Simon, S., 2007. Accelerated carbonation of municipal solid waste incineration fly ashes. Waste Manag. 27, 1200–1206. http://dx.doi.org/10.1016/j.wasman.2006.06.011.

Martín, D., Aparicio, P., Galán, E., 2016. Capture of CO_2 by construction waste. In: Carmina, B., Pasero, M. (Eds.), 2nd European Mineralogical Conference. “Mineral, Rocks and Fluids: Alphabet and Words of Planet Earth”. Abstracts Book. Rimini, Italy, pp. 317.

Metz, B., Davidson, O., De Coninck, H., Loos, M., Meyer, L., IPCC, 2005. IPCC Special Report on Carbon Dioxide Capture and Storage. Intergovernmental Panel on Climate Change, Geneva (Switzerland) (Working Group III).

Montes-Hernandez, G., Pérez-López, R., Renard, F., Nieto, J.M., Charlet, L., 2009. Mineral sequestration of CO_2 by aqueous carbonation of coal combustion fly-ash. J. Hazard. Mater. 161, 1347–1354. http://dx.doi.org/10.1016/j.jhazmat.2008.04.104.

Petschick, R., 2004. MacDiff 4.2.5 [WWW Document]. Inst. Geol. Univ. Erlangen Ger. http://www.geol-pal.uni-frankfurt.de/Staff/Homepages/Petschick/classicsoftware.html#MacDiff.

Petschick, R., 2010. MacDiff 4.2.6. Power Diffraction Software [WWW Document]. http://www.geol-pal.uni-frankfurt.de/Staff/Homepages/Petschick/classicsoftware.html#MacDiff, Accessed date: 1 April 2018.

Seifritz, W., 1990. CO_2 disposal by means of silicates. Nature. http://dx.doi.org/10.1038/345486b0.

Shao, Y., Mirza, M.S., Wu, X., 2006. CO_2 sequestration using calcium-silicate concrete. Can. J. Civ. Eng. 33, 776–784. http://dx.doi.org/10.1139/l05-105.

Stocker, T.F., Qin, D., Plattner, G.K., Tignor, M., Allen, S.K., Boschung, J., Nauels, A., Xia, Y., Bex, V., Midgley, P.M., 2013. IPCC, 2013: summary for policymakers in climate change 2013: the physical science basis. In: Contribution of Working Group I to the Fifth Assessment Report of the Intergovernmental Panel on Climate Change.